JOURNAL OF CATALYSIS **171,** 208–218 (1997)
ARTICLE NO. CA971788

Mechanism of the Selective Catalytic Reduction of NO by NH_3 over MnO_x/Al_2O_3

I. Adsorption and Desorption of the Single Reaction Components

W. Sjoerd Kijlstra, Danny S. Brands, Eduard K. Poels, and Alfred Bliek[1]

Department of Chemical Engineering, University of Amsterdam, Nieuwe Achtergracht 166, 1018 WV Amsterdam, The Netherlands

Received February 27, 1997; revised May 26, 1997; accepted June 2, 1997

The adsorption of NO and NH_3 on MnO_x/Al_2O_3 catalysts, used for the low temperature selective catalytic reduction of NO, was studied separately by use of TPD (with labelled compounds) and FTIR. Besides, the influence of O_2 on the adsorption of the reactants was investigated. At 323 K, NH_3 can adsorb as coordinated NH_3 and ammonium ions, which both have comparable thermal stability. Hence, both of them, as well as amide species, can be present at reaction temperature (423 K). In the presence of O_2 the relative distribution of these three surface species does not change. NO adsorbs in small quantities on the surface of these catalysts after an inert treatment as Mn^{3+}–NO nitrosyls and some nitrites/nitrates. However, it adsorbs in significant amounts after an oxidative pretreatment and in high amounts (NO/Mn $\approx$ 1) in the presence of gas phase O_2. At 423 K, the following compounds can be present, in increasing order of thermodynamic stability: linear nitrites, bridged nitrites, monodentate nitrites < bridged nitrates < bidentate nitrates. The formation of these five species is strongly enhanced in the presence of O_2, and probably proceeds by NO oxidation. In contrast, nitrosylic compounds are unstable in O_2 containing atmospheres. The uptake of NO in the presence of O_2 is lower than the NO_2 uptake, and relatively more stable nitrates are formed in the latter case. The role of O_2 is to oxidise NO at the surface rather than in the gas phase.

INTRODUCTION

Selective catalytic reduction (SCR) of NO with NH_3 is a proven technique for the removal of NO_x from flue gases of stationary sources. A large amount of literature exists on applied and fundamental studies on several SCR catalyst systems. Among them, alumina supported manganese oxides appear to be very active catalysts for this reaction (1–4) in the low temperature range (383–473 K). Hence, they may be considered promising for application in add-on units for existing power plants. At low loadings, the high activity is combined with a very high selectivity towards N_2 production (5).

Recently, Kapteijn *et al.* (6) published some mechanistic aspects of the SCR reaction over these catalysts using FTIR and TP(R)D experiments. They suggest that the reaction proceeds by adsorption of NH_3 on Lewis acid sites, followed (partly) by H-abstraction yielding a NH_2 surface species. This species would react with NO (weakly adsorbed or gaseous), possibly at an octahedral Mn^{3+} site which holds one NO and one NH_3/NH_2, to yield the reaction products. The authors proposed four possible roles of oxygen in the reaction mechanism: (1) gas phase oxidation of NO to NO_2, which adsorbs faster than NO; (2) more readily adsorption of NO on oxidised surfaces, hence enhancing the reaction rate; (3) creation of oxidised sites necessary for H-abstraction of the adsorbed NH_3; (4) reoxidation of the surface to close the catalytic cycle.

Despite the amount of valuable information presented in (6) some crucial aspects of the mechanism remain unclear:

(1) The role of O_2 in the catalytic cycle must be further elucidated. Because Kapteijn *et al.* performed their FTIR studies in the absence of O_2, its role in the formation of reactive intermediates is not yet clarified.

(2) It was not unambiguously established whether the reaction proceeds by a Langmuir Hinshelwood (LH) or an Eley Rideal (ER) mechanism. TPD results point towards direct reaction of gas phase NO (6). In contrast, kinetic studies revealed that the reaction order in NO is broken (4) and changes upon concurrent adsorption of H_2O (3), suggesting a LH mechanism.

(3) Low loaded catalysts deactivate very slowly during the first 200 h in a reaction mixture at 423 K (7). This deactivation calls for an explanation.

These questions, discussed abundantly in mechanistic studies on other SCR catalysts, have to be clarified for the MnO_x/Al_2O_3 catalysts as finally a reaction rate equation based on a reliable mechanistic model, suitable for reactor

[1] To whom correspondence should be addressed. E-mail: bliek@chemeng.chem.uva.nl.

0021-9517/97 $25.00

design purposes, is desired. They will be discussed in the present and subsequent paper.

In literature, a number of active intermediates in the SCR catalytic cycle have been proposed. General agreement merely exists on one point: the reaction starts by (strongly) adsorbed NH_3. Some authors suggest that NH_3 adsorbed as NH_4^+ on Brønsted acid sites is the active species (on V_2O_5/TiO_2 and related systems, e.g. (8–10), on Cu-exchanged zeolite Y(11)), whereas others claim that Lewis acid sites are important to obtain active NH_3-intermediates (on Cu/TiO_2, e.g. (12), on V_2O_5/TiO_2 (13)). When a LH mechanism is suggested a large variety of adsorbed NO complexes is proposed as active intermediates: nitrosyls (6), nitrosonium ion (on Ce/mordenite (14)), several nitrites (on Cu/Al_2O_3 (15), CrO_x/TiO_2 (16) and Cu/MFI (17)) and nitrates (on Cu-ZSM-5 (18) and Cr_2O_3 (19)).

Because of the large number of surface species that can be formed under SCR reaction conditions a detailed, systematic approach is necessary to study the above-mentioned mechanistic questions on MnO_x/Al_2O_3. In this paper we will discuss the way in which NO and NH_3 can adsorb under reaction conditions on pure and supported manganese oxides, with emphasis on the 2 wt% Mn loaded catalysts, using both TPD and *in situ* FTIR experiments. Labelled components are used during TPD to reveal the origin of the formed compounds. Thermal stabilities of the adsorbed species are compared. Also, the role of O_2 on the adsorption of NO and NH_3 and the role of gas phase NO_2 formation are evaluated. Furthermore, it is important to reveal whether the formed surface compounds are located on manganese sites or on the Al_2O_3 support, as catalytic activity is related to Mn centres.

In a subsequent paper the specific role of the formed surface and gas phase compounds with respect to the SCR reaction cycle will be established by use of transient response techniques, TPD (with use of labelled components) and FTIR.

EXPERIMENTAL

Catalysts

The catalysts were prepared by incipient wetness impregnation of a Ketjen CK300 γ-Al_2O_3 support (S_{BET} = 192 $m^2\,g^{-1}$, pore volume 0.5 $cm^3\,g^{-1}$, and particle size 150–250 μm) with an aqueous solution of $(CH_3COO)_2Mn \cdot 4H_2O$. Subsequently, the catalysts were dried in stagnant air overnight at 383 K, followed by calcination in O_2 at 573 K for 1 h and at 773 K for 3 h. Due to the limited solubility of the precursor the impregnation was performed in several steps with drying in-between. In this way, samples were prepared of 2 and 15 wt% manganese loading (S_{BET} of 172 and 150 $m^2\,g^{-1}$, respectively). A more detailed characterisation of these catalysts was reported previously (5, 20). As reference materials both unsupported Mn_2O_3 ($S_{BET} = 36\ m^2\,g^{-1}$), prepared by thermal decomposition of $MnCO_3$ (Aldrich) in air at 823 K, and the γ-Al_2O_3 support were used. These were subjected to the same calcination procedure before use as the supported catalysts.

Gases

Various gases: 0.40 vol% NO/He, 0.75 vol% ^{15}NO/He (99% isotopically pure), 0.40 vol% NH_3/He, O_2 (99.6% purity), 3.5 vol% $^{18}O_2$/He (99% isotopically pure), and He (99.996%) were used during the flow reactor studies (UCAR). The O_2 was dried before use by molecular sieves (5 A, Janssen Chimica). For *in situ* FTIR experiments pure NO (99.9%), NH_3 (99.998%), and O_2 (99.6%) were used (UCAR).

Temperature Programmed Desorption (TPD)

The TPD experiments were performed in a setup described elsewhere (21) containing a flow reactor connected on-line with a mass spectrometer (UTI 100C). The accuracy of the analysis of the MS is within 3–5%. The connecting tubing was heated at 385 K to avoid adsorption on the walls. Each experiment started with a pretreatment in 2 vol% O_2/He or He up to 773 K. In some experiments the pretreatment was performed in 1 vol% $^{18}O_2$/He. Subsequently, the sample, containing 100 mg of 2 wt% Mn/Al_2O_3, was cooled down to 323 K in the same atmosphere and purged with He to remove any physisorbed O_2. After this pretreatment a gas mixture containing 1000 ppm NO (with or without 1 vol% $^{18}O_2$ in He) or 1000 ppm NH_3 in He was passed over the catalysts until saturation of the catalyst surface was reached, as apparent from the MS data. Subsequently, the sample was purged in He for about 60 min to remove all physisorbed species. Finally, TPD was carried out in pure He at a heating rate of 5 K min^{-1} up to 773 K, followed by a 1 h isothermal period. All flow rates were 50 $cm^3\ min^{-1}$. Figures are denoted as follows: pretreatment/adsorption (e.g., $O_2/NO + O_2$ means that pretreatment took place in 2 vol% O_2/He and subsequent adsorption in 1000 ppm NO + 1 vol% O_2). Whenever either the pretreatment or the adsorption step was performed in the presence of labelled O_2, ^{15}NO was used to avoid overlapping MS signals.

Fourier Transform Infrared Spectroscopy (FTIR)

Typically, 15–20 mg of material was pressed in self-supporting discs. A detailed description of the *in situ* infrared transmission cell is given elsewhere (22). Spectra were recorded with a Biorad FTS 45 A spectrometer. To obtain a spectrum with 2 cm^{-1} resolution over the spectral range 4000–1000 cm^{-1} 64 scans were averaged. Samples were *in situ* pretreated *in vacuo* at 673 K for 1 h and subsequently cooled down to 323 K. At this temperature, increasing amounts of NO or NH_3 were adsorbed and spectra were

recorded as a function of both time and partial pressure of the adsorbate. Moreover, co-adsorption of O_2 with either of the reactants was evaluated. The adsorption was followed by evacuation at 323 K and heating up to 673 K *in vacuo*; during heating, spectra were recorded at increments of 25 K.

RESULTS

NH_3 Adsorption

Temperature programmed desorption. The TPD profile of the He/NH_3 experiment for a 2 wt% Mn/Al_2O_3 catalyst is shown in Fig. 1. As reported before for higher Mn loadings (6), NH_3 desorbs in a broad temperature range (350–700 K), characteristic for the presence of several (up to five) adsorbed NH_3 species differing in thermal stability on (low loaded) γ-Al_2O_3 surfaces (23, 24). The amount of NH_3 adsorbed per unit surface area is comparable to higher loaded samples (see Table 1 and Ref. (6)). Conversely, the NH_3/Mn ratio is significantly higher on low loaded samples, suggesting that the Al_2O_3 surface contributes considerably to the NH_3 uptake. In the entire temperature range no N_2 desorption is observed, while only small amounts of H_2O desorb from the surface above 700 K.

Infrared spectroscopy. Adsorption of NH_3 at 323 K followed by evacuation results in a rather complex spectrum (Fig. 2), reflecting the complex chemistry of NH_3 interaction with oxidic surfaces. On γ-Al_2O_3, bands can be found at 1610–1620 cm^{-1} and 1190–1290 cm^{-1} (assigned to the asymmetric and symmetric deformation, respectively, of coordinated NH_3 on Lewis acid sites), 1479 and 1690 cm^{-1} (assigned to asymmetric and symmetric deformation, respectively, of ammonium ions, resulting from NH_3 adsorption on Brønsted acid sites). Moreover, a small shoulder around 1510 cm^{-1}, attributed to an amide (NH_2) species (scissoring mode) (25, 26), is observed. At 2 wt% Mn loading, the band due to symmetric deformation of coordinated NH_3 shifts to lower wavenumber and contains an additional component at about 1190 cm^{-1}. This band is also found in the spectrum of unsupported Mn_2O_3, together with absorptions at 1220 and 1130 cm^{-1}; all of them are attributed to adsorption on different Lewis acid Mn^{3+} sites. Unsupported Mn_2O_3 shows a very small peak due to ammonium ions (1459 cm^{-1}), whereas the band due to amide species is relatively strong and centred at 1530 cm^{-1}. Correspondingly, bands are found in the NH stretching region at 3400, 3358, 3263, and 3143 cm^{-1} (not shown). The 2 and 15 wt% loaded catalysts show a band due to ammonium ions composed of two components, at 1479 and 1459 cm^{-1}, resulting from adsorption at Al_2O_3 and Mn-sites, respectively. When

TABLE 1

Amounts Desorbed during TPD after Adsorption at 323 K; 2 wt% Mn/Al_2O_3

TPD	Compound	10^{-6} moles m^{-2}	Moles/moles Mn
He/NH_3	NH_3	2.16	1.02
He/NO	NO	0.033	0.016
$^{18}O_2/^{15}NO$	^{15}NO (450 K)	0.126	0.060
$^{18}O_2/^{15}NO$	$^{15}N^{18}O$ (450 K)	0.018	0.008
$^{18}O_2/^{15}NO$	^{15}NO (645 K)	0.167	0.079
$^{18}O_2/^{15}NO$	$^{15}N^{18}O$ (645 K)	0.030	0.014
$^{18}O_2/^{15}NO$	$^{16}O_2$ (650 K)	0.056	0.026
$^{18}O_2/^{15}NO$	$^{16}O^{18}O$ (650 K)	0.008	0.004
He/NO_2	$NO_{(2)}$ (400 K)	0.65	0.30
He/NO_2	$NO_{(2)}$ (600 K)	2.32	1.09
He/NO_2	O_2 (600 K)	1.12	0.53

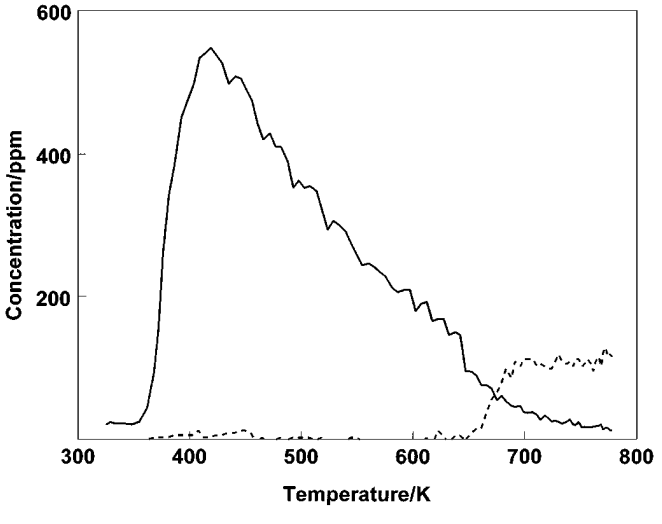

FIG. 1. TPD NH_3/He after adsorption at 323 K; NH_3 (———) and H_2O (– – –); 2 wt% Mn/Al_2O_3.

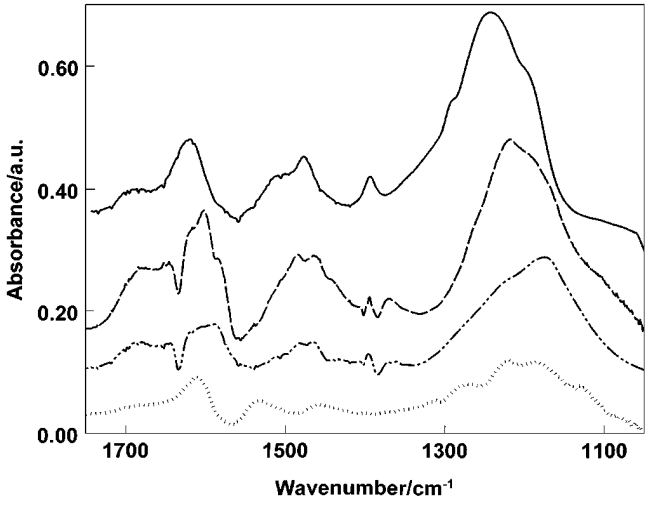

FIG. 2. IR-spectra after adsorption 2 mbar NH_3 at 323 K followed by evacuation: γ-Al_2O_3 (———); 2 wt% Mn/Al_2O_3 (– – –); 15 wt% Mn/Al_2O_3 (—·—); Mn_2O_3 (·····).

the spectra in Fig. 2 are compared it is clear that the relative content of NH_3 adsorbed on Brønsted acid sites decreases with loading, whereas the relative content of NH_2-species increases. In the hydroxyl region of the spectra (not shown) the bands due to basic, neutral, and acidic hydroxyls (centred at 3770, 3725, and 3680 cm^{-1}, respectively (27)) decrease (especially the basic one), possibly by H-bridging with NH_3 molecules adsorbed on adjacent sites. This perturbation is most clearly observed at the lowest Mn loading and the γ-Al_2O_3 support. The spectrum observed after NH_3 adsorption and subsequent admission of O_2 at 323 K is comparable to that after NH_3 adsorption, indicating that O_2 does not change the relative distribution of adsorbed NH_3 species.

It should be noted that the formation of all above-mentioned surface compounds proceeds very rapidly; spectra following adsorption during 0.5 min exactly match spectra after adsorption during 10 min. The lower intensity of the Mn_2O_3 sample compared to the supported catalysts is due to the lower surface area (and by consequence a lower concentration of surface compounds) of this sample (28).

After adsorption and subsequent evacuation the samples were heated to 673 K, with spectra recorded at increments of 50 K. As an example, some spectra of the 2 wt% Mn/Al_2O_3 are shown in Fig. 3. All bands progressively decrease in intensity between 323 and 573 K, except for the shoulder due to NH_2 species, the relative intensity of which increases slightly up to 373 K, followed by decreasing intensity at higher temperatures. This indicates that heating to temperatures slightly above 323 K is enough to activate adsorbed NH_3 to form NH_2 species. Clearly, there is no significant difference in thermodynamic stability between NH_3 molecules adsorbed on Lewis and Brønsted acid sites.

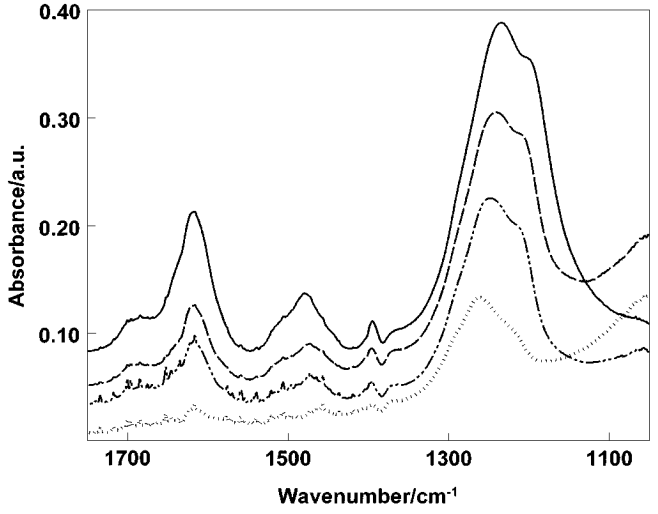

FIG. 3. IR-spectra after adsorption 2 mbar NH_3 at 323 K, followed by evacuation (———), and subsequent heating to 373 K (– – –), 423 K (—·—), and 523 K (ıllıllıll); 2 wt% Mn/Al_2O_3.

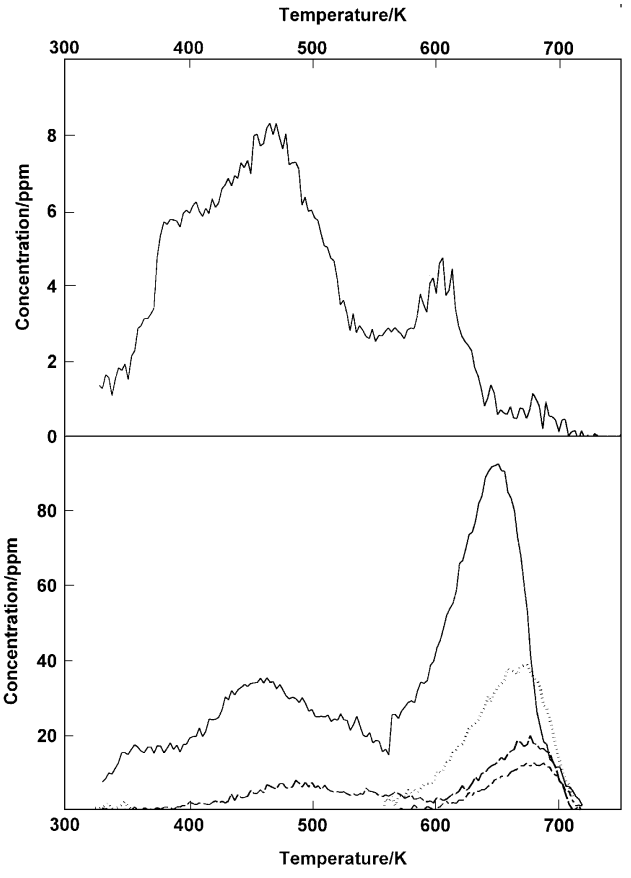

FIG. 4. TPD after adsorption at 323 K: *upper* He/NO; *bottom* $^{18}O_2$/NO; ^{15}NO (———); $^{15}N^{18}O$ (– – –); $^{16}O_2$ (ıllıllıll); and $^{16}O + {}^{18}O$ (— — — —); 2 wt% Mn/Al_2O_3.

NO Adsorption

Temperature programmed desorption. When 2 wt% Mn/Al_2O_3 is pretreated in inert atmosphere, the adsorption of NO in the *absence* of O_2 is very limited (see Fig. 4a); two small peaks are observed during TPD at 480 and 600 K. In contrast, after a pretreatment in 2 vol% O_2/He the amount of adsorbed NO is about 10 times higher; $^{18}O_2$ was used to reveal the origin of the oxygen atoms during desorption. In the TPD pattern in Fig. 4b two desorption peaks are observed, a broad peak in the low temperature range, centred at 450 K (*LT-peak*), and a strong peak at higher temperature, with a maximum at 645 K (*HT-peak*). A minor fraction of the desorbing NO has exchanged its O atom with the $^{18}O_2$ pretreated surface. This second peak is accompanied by desorption of $^{16}O_2$ and a small amount of $^{16}O^{18}O$. It should be noted that NO_2 cannot be observed due to fragmentation in the mass spectrometer. Hence, the observed NO may originate from NO_2. No desorption of N_2 is observed over the entire temperature range. All desorbed quantities are presented in Table 1.

When adsorption of NO is carried out in the presence of O_2 significantly larger amounts are adsorbed (Fig. 5 and

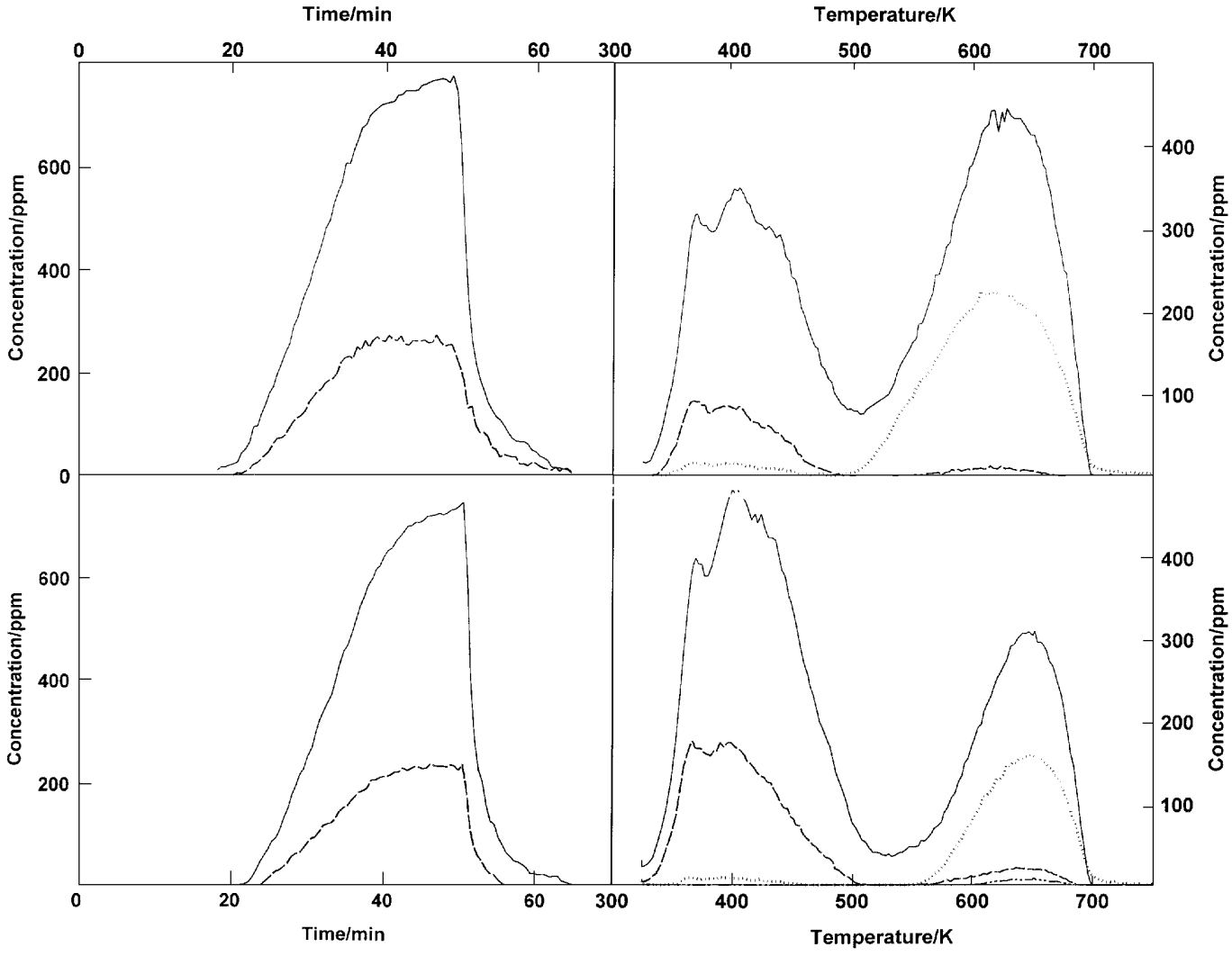

FIG. 5. *Left*: breakthrough curves during adsorption NO in the presence of O_2 at 323 K: ^{15}NO (———); $^{15}N^{18}O$ (– – –); and $^{16}O_2$ (ıllıllı); *upper*, $O_2/^{15}NO + {}^{18}O_2$; *bottom*, $He/^{15}NO + {}^{18}O_2$. *Right*: TPD after adsorption at 323 K: *upper*, $O_2/^{15}NO + {}^{18}O_2$; *bottom*, $He/^{15}NO + {}^{18}O_2$; ^{15}NO (———), $^{15}N^{18}O$ (– – –), and $^{16}O_2$ (ıllıllı); 2 wt% Mn/Al_2O_3.

Table 2). To reveal the origin of the oxygen atoms that desorb after NO/O_2 coadsorption, $^{18}O_2$ was used during adsorption (*not* during pretreatment). The NO breakthrough patterns preceding the desorption experiments (Fig. 5a) show up to 250 ppm of $^{15}N^{18}O$ at breakthrough. This species can result either from O-exchange with adsorbed oxygen species or from fragmentation of produced NO_2. In the latter case, this means that about 50% of the NO (= 500 ppm) is converted to NO_2 as $^{15}N^{16}O^{18}O$ which is fragmented in the mass spectrometer to equal amounts of $^{15}N^{16}O$ and $^{15}N^{18}O$. As reference, the breakthrough curve of ^{15}NO in the presence of $^{18}O_2$ was measured in an empty reactor, leading to 25–35 ppm $^{15}N^{18}O$ in the reactor outlet, corresponding to 5–7% NO conversion. Hence, gas phase NO oxidation hardly contributes to the 50% NO conversion observed in the breakthrough curves over MnO_x/Al_2O_3. Clearly, gas phase NO oxidation occurs to a small extent to the temperature of the heated tubing (400 K). Again, desorption of NO proceeds in two temperature regions giving a LT-peak (at 410 K) and a HT-peak (at 600 K), although both peaks seem to be composed of more than one species. No N_2 desorption is observed over the entire temperature range. For a pretreatment in He the LT-peak is larger than the HT-peak, whereas the opposite is true for a pretreatment in O_2. Apparently, a preoxidised surface favours the formation of thermally stable NO containing surface complexes. The low temperature ^{15}NO desorption is accompanied by desorption of $^{15}N^{18}O$. Hence, gas phase O_2 is partly involved in the adsorption of the low temperature mode of NO. In contrast, hardly any $^{15}N^{18}O$ desorbs at temperatures above 550 K. It is remarkable that desorption of NO at these temperatures is accompanied by desorption of unlabeled O_2,

TABLE 2

Amounts Desorbed during TPD after Adsorption ^{15}NO and $^{18}O_2$ at 323 K; 2 wt% Mn/Al_2O_3

Pretreatment	Compound	10^{-6} moles m^{-2}	Moles/moles Mn
He	$^{15}N^{18}O$ (400 K)	0.363	0.17
He	$^{15}N^{18}O$ (615 K)	0.035	0.02
He	$^{15}N^{16}O$ (400 K)	1.14	0.54
He	$^{15}N^{16}O$ (615 K)	0.648	0.31
He	$^{16}O_2$ (615 K)	0.318	0.15
$^{18}O_2$	$^{15}N^{18}O$ (400 K)	0.164	0.08
$^{18}O_2$	$^{15}N^{18}O$ (615 K)	0.016	0.01
$^{18}O_2$	$^{15}N^{16}O$ (400 K)	0.816	0.39
$^{18}O_2$	$^{15}N^{16}O$ (615 K)	1.17	0.55
$^{18}O_2$	$^{16}O_2$ (615 K)	0.622	0.29

which is not found in reference TPD experiments without NO adsorption. The observed ratio of $NO/O_2 \approx 2$ corresponds to decomposition and complete desorption of a nitrate species. The results suggest that gas phase O_2 is not directly involved in the formation of thermally stable NO complexes, despite increased NO adsorption in its presence.

Finally, the desorption profiles after adsorption of NO in the presence of O_2 are compared with the profiles after adsorption of NO_2 (Fig. 6). Due to fragmentation of NO_2 only NO and O_2 are detected. The uptake of NO_2 is about 40% higher than the NO uptake in the presence of O_2. The desorption profile shows again a LT peak and a HT peak, but compared with the profiles after adsorption of NO and O_2, a higher amount of stable NO surface complexes are formed.

Infrared spectroscopy. Spectra of the adsorption of NO in the absence and presence of O_2 are shown in Fig. 7. The

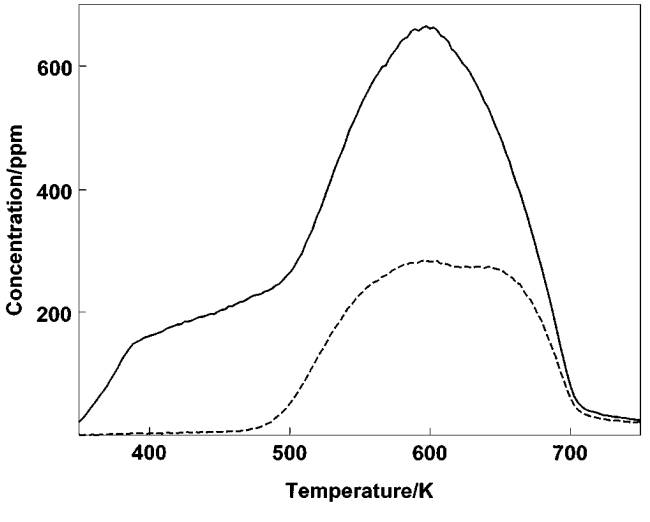

FIG. 6. TPD NO_2/He after adsorption at 323 K; NO (———), and O_2 (– – –); 2 wt% Mn/Al_2O_3.

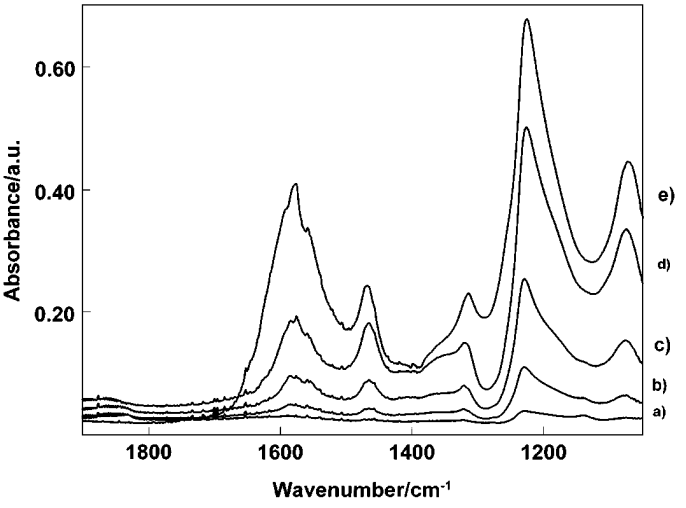

FIG. 7. IR spectra at 323 K after adsorption (a) 1 mbar NO, (b) +10 min, (c) +1 mbar NO, (d) +5 mbar O_2, and (e) prolonged O_2 adsorption followed by evacuation; 2 wt% Mn/Al_2O_3.

partial pressures of both reactants are in the same order of magnitude as those used during the TPD experiments. Upon admission of 1 mbar NO, two weak bands can be observed due to mono nitrosylic species at 1835 and 1864 cm^{-1}. Previously, the appearance of two bands was attributed to Mn^{3+} species lacking one and zero coordinations, respectively, after adsorption (6). The shift of the mononitrosyl bands to lower frequencies with respect to gaseous NO (1876 cm^{-1}) is due to electron donation from (partly) filled *d*-orbitals of Mn^{n+} to π^*-orbitals of NO. Furthermore, a strong band appears at 1230 cm^{-1}, together with weaker bands at 1136, 1322, 1465, and 1586 cm^{-1} due to several nitrite and nitrate species. As hardly any reference material on MnO_x/Al_2O_3 systems has been published, these bands are assigned using both literature on inorganic Mn containing complexes and $NO(+O_2)/NO_2$ adsorption studies on amorphous, oxidic surfaces of other transition metals. According to studies on MgO (29), the band at 1136 cm^{-1} can be assigned to chelating (bidentate) nitrites (see also Table 3). The band at 1465 cm^{-1} can be assigned to the ν_3 stretch vibration of a linearly coordinated nitrite, as observed on a variety of other oxides (16, 30–32), among which Al_2O_3 (30). Two assignments can be suggested for the band at 1322 cm^{-1}. Centi *et al*. (30) also observed this band on Al_2O_3 and assigned it to linear nitrites. On the other hand, bands in the region 1315–1350 cm^{-1} have been found on several oxidic systems (16, 31–34) and attributed to a M^{n+}–NO_2 species. As linear nitrites are generally characterised in IR by bands at 1466 and 1060 cm^{-1} (31, 32), it is more plausible to assign the band at 1322 cm^{-1} in our spectra to a M^{n+}–NO_2 species. The relatively strong band at 1230 cm^{-1} can be attributed to bridged nitrites (30–32). The band at 1586 cm^{-1} can be reasonably assigned to one

TABLE 3

Thermal Stabilities Adsorbed NO Complexes

Species	ν_3/cm^{-1}	ν_3/cm^{-1}		Desorption/ decomposition
Nitrosyl	1835		$Mn^{n+}-N=O^{\delta-}$	323 K
Bridged nitrate	1620	1220	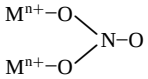	423–573 K
Bidentate nitrate 'type II'	1290	1555	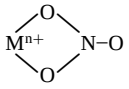	573–698 K
Bridged nitrate 'type I'	1580	1220	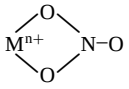	473–573 K
Linear nitrite	1466	1075 (ν_1)	$Mn^{n+}-O-N=O$	323–473 K
Monodentate nitrite	1415	1322 (ν_1)	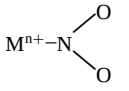	323–473 K
Bridged nitrite		1230	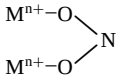	323–523 K

of the split ν_3 vibrations of bidentate nitrate species. As no band is observed in the 1260–1300 cm^{-1} region, the corresponding ν_3 possibly overlaps with the band centred near 1230 cm^{-1}. Hence, both bands can be attributed to a "type I" bidentate nitrate; according to the classification of Schraml-Marth *et al*. (33) on CrO_x. These authors classified bidentate nitrates in different types on the basis of thermal stability, but it is not clear which chemical features give rise to these differences. All bands grow considerably in intensity upon prolonged adsorption, except for the bands at 1835 cm^{-1} and 1136 cm^{-1}. The latter is transformed to a shoulder of the band at 1230 cm^{-1}. A new band appears at 1075 cm^{-1}, which is most reasonably assigned to the ν_1 stretch vibration of linearly coordinated nitrite (31, 32). After adsorption of 2 mbar NO all bands grow further, except for the bands due to nitrosyls. The band at 1586 cm^{-1} clearly contains a second component around 1555–1560 cm^{-1}. Hence, an additional bidentate nitrate is formed, of the "type II" form (33), the matching ν_3 of which, expected at 1260–1300 cm^{-1}, is possibly masked by the band at 1230 cm^{-1}.

Admission of O_2 causes a strong increase in intensity of all nitrite and nitrate bands. The bands of bidentate nitrates contain a third component (maxima at 1585, 1576, and 1560 cm^{-1}) with a shoulder at higher wavenumber attributed to the split ν_3 vibration of bridged nitrates (13, 19, 31–33, 35); the corresponding ν_3 of the latter species is expected in the 1200–1230 cm^{-1} region (31, 32) and probably overlaps with the band at 1230 cm^{-1}. The ν_3 and ν_1 due to linear nitrites are centred at 1466 and 1075 cm^{-1}, respectively. A sharp negative peak becomes visible at 3770 cm^{-1} (not shown), representing an interaction of the basic hydroxyls at the surface with NO, possibly adsorbed on adjacent sites by H-bridging (33). The bands of the nitrosylic species are the only ones that are lowered in intensity upon O_2 addition. After prolonged adsorption time (10 min), followed by evacuation, all bands in the spectrum are intensified, except for the nitrosylic bands which have totally disappeared (Fig. 7e). Hence, all detected nitrite and nitrate species are resistant towards evacuation. Separate experiments (not shown) show clearly that bidentate nitrate "type II" species (at 1550–1590 and 1260–1305 cm^{-1}) become predominant at both longer contact times or higher partial pressures of NO and O_2.

Upon heating to 373 K, the bands at 1074, 1230, 1319, and 1466 cm^{-1} decrease in intensity (Fig. 8), whereas more pronounced absorption at 1293 cm^{-1}, assigned to the ν_3 vibration of bidentate nitrate "type II" species, becomes visible. Concurrently, the bands at 1550–1600 cm^{-1} slightly intensify, especially the component at 1555 cm^{-1}. At 423 K, the bands at 1074, 1230, and 1466 cm^{-1} are further reduced indicating that linear nitrites and bridged nitrites desorb/decompose around this temperature, whereas the band at 1293 cm^{-1} becomes stronger. Moreover, the band at 1230 cm^{-1} exhibits a shoulder at higher wavenumber (1260 cm^{-1}). The bands at 1550–1600 cm^{-1} remain unchanged at this temperature, while the shoulder around 1620 cm^{-1} is much weaker, which means that decomposition of bridged nitrates starts around this temperature. At 473 K, the bands at 1074 and 1466 cm^{-1} have disappeared. The band at 1230 cm^{-1} is reduced and is slightly shifted towards 1233 cm^{-1}. The band at 1294 cm^{-1} and the shoulder at 1260 cm^{-1} become more intense, while the nitrate band at 1580 cm^{-1} is unchanged and the component at 1555 cm^{-1} even

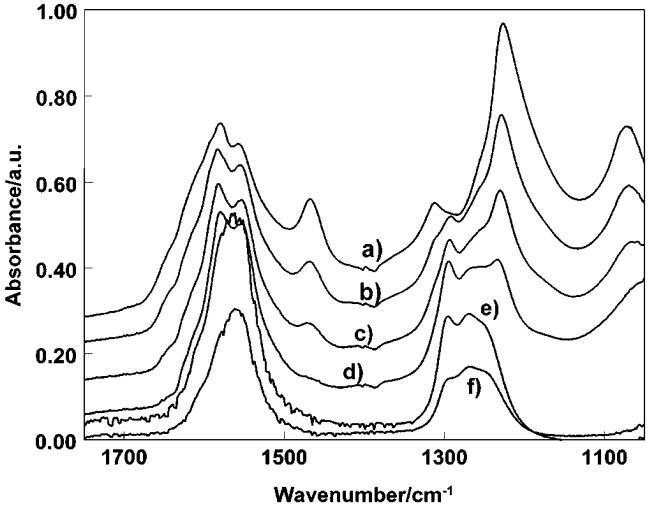

FIG. 8. IR spectra after adsorption NO and O_2 at 323 K followed by evacuation (a) at 323 K, and heating to (b) 373 K, (c) 423 K, (d) 473 K, (e) 573 K, and (f) 673 K; 2 wt% Mn/Al_2O_3.

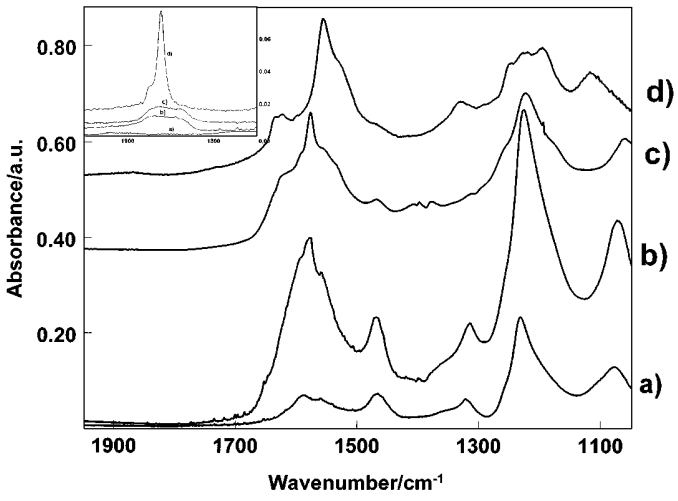

FIG. 9. IR spectra after adsorption NO and O_2 at 323 K at (a) γ-Al_2O_3, (b) 2 wt% Mn/Al_2O_3, (c) 15 wt% Mn/Al_2O_3, and (d) Mn_2O_3.

becomes stronger. This indicates that bidentate nitrates are formed during heating at the expense of less stable nitrites and nitrates. At 573 K, the spectrum exists of a doublet at 1580 and 1555 cm^{-1} and a doublet at 1294 and 1269 cm^{-1}, indicating that at this temperature mainly bidentate nitrates are present at the surface. Subsequent adsorption of NO and O_2 at 573 K (not shown) yields the same spectrum. The doublets are significantly reduced in intensity at 673 K, whereas all NO containing surface compounds are removed upon 1 h evacuation at 698 K.

Figure 9 shows the spectra after NO adsorption as a function of Mn content. The amount of nitrosylic species (bands at 1862 and 1835 cm^{-1}) formed upon adsorption of 2 mbar NO at 323 K (insert, Fig. 9), decreases with Mn loading. Previous experiments (6) already showed that the band at 1860 cm^{-1} grows with increasing adsorption time at the expense of the band at a lower wavenumber. At the pure Al_2O_3 support NO does not adsorb to form nitrosyls. Prolonged NO adsorption, followed by O_2 admission and evacuation yields the spectra shown in Fig. 9. Unsupported Mn_2O_3 exhibits a distinct band due to the ν_3 of bridged nitrates at 1627 cm^{-1} and a sharp band attributed to the ν_3 of bidentate nitrates "type II" at 1556 cm^{-1}. Both species have their corresponding ν_3 in the triplet band in the region 1200–1280 cm^{-1}. Moreover, the band attributed to monodentate nitrite species is clearly observed at 1328 cm^{-1}. In contrast to the supported manganese oxides and the pure support, no bands are observed at 1466 cm^{-1} and below 1100 cm^{-1}. On the other hand, an additional band is observed at 1115 cm^{-1}, which can be attributed to chelating nitrites (29). In general, the bands at 1466 and 1320 cm^{-1} decrease with increasing Mn content. Furthermore, it is clear that Mn sites are involved in the formation of bidentate nitrates "type II" (1558 cm^{-1}).

DISCUSSION

Location of Adsorbed Species on Supported Manganese Oxides

Low loaded ($\leq$2 wt%) alumina supported manganese oxides contain isolated Mn^{3+} sites and small, well dispersed MnO_x clusters, in which the oxidation state of the Mn is mainly 3+ (5). A monolayer coverage is reached at 8.4 wt%; by consequence, a large part of the exposed surface of low loaded catalysts is γ-Al_2O_3. As catalytic activity is related to the presence of Mn it is important to understand whether adsorbed species are located only on Mn sites, on the support or on both.

Upon NH_3 adsorption both NH_4^+ ions and coordinated NH_3 are formed. An increase in Mn content results in decreased formation of NH_4^+ ions and increased formation of NH_2 species. Due to the simultaneous occurrence of both trends at higher loadings, it is not likely that the formed NH_2 results from disproportionation of coordinated NH_3, according to: $2\ NH_3 \rightleftharpoons NH_4 + NH_2$, as was proposed previously (6). Formation of NH_2 species by hydrogen abstraction from coordinated NH_3, as observed on many other oxidic systems (12, 25), is more likely. A previous characterisation study on alumina supported manganese oxides (5) provides evidence for the reaction of OH groups of the Al_2O_3 with the manganese precursor molecule during impregnation. The observed decrease in NH_4^+ species with Mn loading is in good agreement with these data. Hence, at the Mn^{3+} sites NH_3 is preferentially adsorbed as coordinated NH_3 although formation of $Mn(NH_3)_x$ species ($x > 1$) cannot be excluded as, for instance, spectra of the $[Mn(NH_3)_6]^{2+}$ complex show an IR band on 1134 cm^{-1} (36).

Upon NO adsorption, neither of the nitrosylic species is observed on the bare γ-Al_2O_3 support, in line with work presented by Centi *et al.* (30). Hence, the observed nitrosyls can be described as Mn^{3+}–NO species usually indicated with a negative charge at the NO resulting from electron donation from *d*-orbitals of the Mn atom to π^* orbitals of the NO molecule.

In general, for both supported and unsupported manganese oxides NO adsorption occurs predominantly on oxygen atoms rather than metal atoms, thus giving rise to a variety of nitrite and nitrate species.

The nitrite band observed at 1115 cm^{-1} is another feature which is due to species located exclusively at MnO_x sites (Fig. 9). However, as this band is not found in the spectra of the supported catalysts, not even for the highest loading, it is likely that this species is absent on low loaded Mn catalysts.

Linearly coordinated nitrite is not observed at unsupported Mn_2O_3, whereas its bands are seen in the spectra of all Al_2O_3 containing samples. Its intensity decreases with Mn loading. Hence it is reasonable to presume that these species are formed exclusively on the Al_2O_3 surface.

Bidentate nitrates are observed for all investigated samples. At unsupported Mn_2O_3 the "type II" form (according to the classification presented in (33); bands at 1555 and 1260–1300 cm^{-1}) is the only form observed. On the Al_2O_3 containing samples all three forms of bidentate nitrates are formed and broad bands in the 1550–1600 cm^{-1} region are found.

Bridged nitrates are also observed on all investigated samples. However, their content seems to increase with Mn loading. Hence, it is reasonable to assume that formation of these nitrates occurs on the Al_2O_3 surface, the Mn_2O_3 surface, and at the interface, with one Mn and one Al atom. The relative content of the various formed nitrates seems to be independent of Mn loading, in contrast to results for the CuO/Al_2O_3 system (30), where increasing nitrate formation was observed with Cu loading. The same holds for the formation of bridged nitrites (band around 1230 cm^{-1}).

As monodentate nitrites are found on all investigated samples they are supposed to be present on both Al and Mn sites of supported catalysts.

Thermal Stability of the Formed Surface Compounds

The TPD profiles after NH_3 adsorption show that the thermodynamic stability of the formed compounds varies considerably. IR spectra reveal that NH_4^+ ions as well as coordinated NH_3 progressively desorb over the entire temperature range 323–573 K. Hence, the TPD peak cannot be split in a part with mainly NH_4^+ desorption and one representing desorption of coordinated NH_3 desorption. Formation of NH_2 species is slightly enhanced during the first part of the heating interval (up to 373 K), whereas its content decreases at higher temperatures. Hence, in the absence of NO both NH_4^+ and coordinated NH_3, as well as some NH_2 species, are present at reaction temperature (423 K) at the surface of low-loaded Mn catalysts.

From the TPD profiles it is clear that the adsorbed NO surface compounds can be divided into two modes with respect to their thermal stability. The fine structure in both peaks indicate that each is composed of more than one NO complex, which agrees with the observation of six adsorbed NO species in the IR spectra. According to these IR results, the most thermodynamically stable compound is the bidentate nitrate "type II" species. For a variety of other oxidic catalytic systems (30, 33) this complex is found to be the most stable one. Thus, the high temperature peak (HT peak) of the TPD profiles must at least partly be due to the decomposition of this complex. Bidentate nitrates "type I" (band 1584 cm^{-1}) mainly decompose between 473 and 573 K, thus are less stable than the "type II" species, in agreement with results on CrO_x (33). Bridged nitrates are observed in the IR spectra up to 523 K, thus must be present in the HT TPD peak as well. As the bands due to linearly coordinated nitrates, monodentate nitrites and bridged nitrites decrease in intensity in the spectra recorded at 348–423 K, these species are likely desorbing in the low temperature peak (LT peak) of the TPD profiles. Nitrosylic species also fall in the category of weakly adsorbed species as they disappear readily upon evacuation at 323 K. However, as the bands of nitrosyls decrease upon admission of oxygen, they are apparently unstable in gas streams containing 2 vol% O_2 and thus are not part of the LT peak of the TPD profiles shown in Fig. 5. The significant role that was attributed to nitrosyls in the mechanism of the SCR reaction by Kapteijn *et al.* (6) is, by consequence, very doubtful. A summary of the thermal stabilities is presented in Table 3. The IR spectra reveal that bidentate nitrates, although present in small amounts after adsorption of NO and O_2 at 323 K, are also formed during heating. Hence, part of bidentate nitrates originate from weakly adsorbed NO complexes and are formed by (1) readsorption after desorption at lower temperature or (2) a surface reaction.

In summary, in the absence of NH_3, but in the presence of O_2, the NO containing species supposed to be present at the surface of low loaded Mn/Al_2O_3 catalysts at reaction temperature (423 K), are in increasing order of stability: linearly coordinated nitrites, monodentate nitrites, bridged nitrites, bridged nitrates, and bidentate nitrates.

Role of O_2 during NO and NH_3 Adsorption

When both the pretreatment and the adsorption of NO at low loaded Mn/Al_2O_3 catalysts are performed in the absence of O_2 few NO molecules adsorb on the surface. Pretreatment in O_2 increases the amount of reactive oxygen atoms at the surface resulting in enhanced NO adsorption. If O_2 is present during NO adsorption, large amounts of NO complexes are formed. Recently, Eguchi *et al.* (37, 38), studying the reversible adsorption of NO on mixed Mn–Zr oxide systems, also found a strong enhancement of the adsorption capacity for NO due to the presence of gas phase O_2. Comparable effects of O_2 on the NO adsorption were also reported on CuO/Al_2O_3 catalysts (15). Moreover, the formation of thermally stable complexes is favoured if the pretreatment is performed in O_2. IR results confirm this: O_2 accelerates the formation of all adsorbed NO complexes, except nitrosylic compounds. Especially, the formation of bidentate nitrates is favoured by O_2. NO_2 adsorbs more readily on the surface than NO does, even if the latter is adsorbed in the presence of O_2. Upon NO_2 adsorption, formation of bidentate nitrates and bridged nitrates is enhanced with respect to less stable NO surface complexes.

The breakthrough curves at 323 K of ^{15}NO and $^{18}O_2$ show large amounts of $^{15}N^{18}O$, which can result from (1) oxygen exchange or (2) NO oxidation followed by fragmentation of NO_2 in the MS. Oxygen exchange ($^{15}N^{16}O \rightarrow {}^{15}N^{18}O$) was reported on a variety of oxidic systems (39–41) but always at temperatures above 600 K. Hence, the observed formation of $^{15}N^{18}O$ is more likely explained by NO oxidation; the NO_2 formed is completely adsorbed giving rise to sharp

breakthrough curves. Reference breakthrough curves in an empty reactor show that gas phase NO oxidation only contributes to a small extent to the observed NO_2 formation. Therefore, it can be concluded that gas phase oxidation of NO, one of the roles of O_2 in the selective catalytic reduction of NO as proposed by Kapteijn *et al.* (6), cannot contribute significantly to the overall reaction under the applied conditions. Eguchi *et al.* (37, 38) reported Mn oxides to be very active catalysts for NO oxidation even at temperatures as low as 373 K, which is in agreement with the breakthrough data in Fig. 5.

Despite its significant formation upon adsorption, $^{15}N^{18}O$ only desorbs in small amounts in the LT peak of the TPD profiles. The ratio $^{15}N^{18}O$/Mn is 0.08, whereas the total NO/Mn ratio of the LT peak is 0.47; this means that only one-third of the LT peak can be due to desorption of NO_2.

A second role of O_2, as proposed by Kapteijn *et al.* (6), is the creation of a more oxidised surface, enhancing NO adsorption. This role is confirmed more clearly by the present results. Enhanced NO adsorption after a pretreatment in oxidising atmosphere can thus be explained. Besides, this role of O_2 can explain the accelerated NO adsorption in the presence of gas phase $^{18}O_2$ without the appearance of 50% ^{18}O in the desorption products. The formation of linear nitrites, mainly on Al_2O_3, can be visualised by adsorption of $^{18}O_2$ at the surface followed by NO adsorption. As the oxygen atoms in this complex are not equivalent, no ^{18}O appears in the desorbing NO. Simultaneous formation of bridged nitrites, with two equal O atoms, can account for some desorption of $^{15}N^{18}O$ at low temperatures. Niiyama *et al.* (42), studying the NO adsorption on amorphous chromia, explained the exchange of oxygen in the desorbed NO at low temperature by a surface equilibrium between linear nitrites and bidentate nitrites. Possibly, this equilibrium can also be established between linear nitrites and bridged nitrites. Bridged nitrates and bidentate nitrates also contain nonterminal oxygen atoms which are not equivalent. If these compounds are formed on a surface partly covered by ^{18}O, labelled oxygen is expected in the NO/NO_2 or in desorbing molecular O_2. However, the amount of ^{18}O desorbing in the HT peak is negligible, while a large amount of $^{16}O_2$ desorbs simultaneously with the HT NO peak, in a ratio $NO/O_2 \approx 2$. Hence, the formed bidentate nitrates contain no ^{18}O, whereas their formation is strongly enhanced by the presence of gas phase $^{(18)}O_2$. An explanation for this phenomenon is O-exchange of the ^{18}O atoms with ^{16}O atoms in the upper and subsurface layer in the temperature region of the HT peak. Boreskov (43) reported significant O-exchange reaction rates for pure MnO_2 at temperatures higher than 475 K. Recently, Chang and McCarty (44) showed that exchange of O atoms from NO with lattice oxygen can occur on ZSM-5 based catalysts at temperatures above 523 K. Oxygen-exchange experiments on the 2 wt% Mn/Al_2O_3 did indeed show some formation of $^{16}O^{18}O$ and $^{16}O_2$ at 600 K (not shown), but the exchange rate is too low to result in complete exchange of oxygen with preadsorbed oxygen or lattice oxygen (and thus desorption of $^{16}O_2$ during decomposition of the nitrates). Nevertheless, a higher degree of O-exchange can possibly be established, as ^{18}O atoms are bound more strongly to the surface in the nitrate complexes than in the form of O adatoms resulting in higher surface coverages with ^{18}O. At higher temperatures these ^{18}O atoms do not desorb, but remain at the surface as part of these nitrate complexes and can exchange with preadsorbed or lattice oxygen up to the temperature of nitrate decomposition. An alternative explanation could be that NO can only adsorb as nitrate through bonding with lattice oxygens, thus lossening these from the oxide, if gas phase O_2 adsorbs in the vicinity to compensate for this effect. At present, no definitive explanation can be given for this phenomenon. The appearance of a molecular oxygen peak simultaneously with the HT peak, as observed previously for other SCR catalysts (45–47), is explained by decomposition of nitrate species, leaving reduced metal atoms on the catalytic surface. Unfortunately, no labelled experiments were performed by these authors and thus the origin of the O atoms involved in the nitrate formation remains unknown. The TPD profile after NO adsorption on CuO/Al_2O_3, reported by Sadykov *et al.* (48) is comparable to the one presented in Fig. 5. It shows NO_2 desorption simultaneously with the HT peak of NO, suggesting that the O_2 desorption observed in this study is due to NO_2 desorption and fragmentation in the MS.

The fact that hardly any N_2 desorption is observed during both breakthrough and TPD indicates that NO decomposition does not readily occur at low temperatures on this catalyst.

Previous TPD experiments (6) already showed that the amount of NH_3 that adsorbs hardly depends on the presence of O_2, which is confirmed by the IR spectra in this work that do not show enhanced intensity of the bands due to adsorbed NH_3 species upon subsequent O_2 admission. Besides, the relative distribution of coordinated NH_3, NH_4^+ ions and NH_2 species is not changed by coadsorption of O_2 at these low temperatures. The role of O_2 appears therefore not to be crucial with respect to the adsorption of NH_3.

CONCLUSIONS

The adsorption of NO and NH_3 at the surface of Al_2O_3 supported manganese oxides was studied by FTIR and TPD (using labelled compounds) to determine which surface complexes may be present during reaction conditions for the selective catalytic reduction of NO.

Upon NO adsorption, nitrosylic species are formed at Mn^{3+} sites in the absence of O_2, but they are very unstable in its presence. By consequence, they are no active reactive intermediates over these catalysts. In contrast, at

423 K the NO complexes which are sufficiently stable in the presence of O_2, are at increasing order of thermodynamic stability: linear nitrites, bridged nitrites, monodentate nitrites < bridged nitrates < bidentate nitrates. The formation of these five species is strongly enhanced by the presence of gas phase O_2. Labelling studies reveal that formation of gas phase NO_2 followed by adsorption is, at these low temperatures, only a minor route to the formation of surface species. Creation of additional reactive surface oxygen species, followed by NO oxidation, appears to be the main role of O_2 to establish high NO coverages.

Upon NH_3 adsorption, ammonium ions and coordinated NH_3 are formed. Simultaneously, some adsorbed NH_3 is transformed to NH_2 surface species. No significant differences between the thermal stabilities of these species could be established. Higher Mn loadings tend to favour coordination of NH_3 with subsequent transformation to NH_2 rather than NH_4^+ formation. No evidence was obtained for changes in the distribution of adsorbed NH_3 species by gas phase O_2 at low temperatures.

The role of these adsorbed species with respect to the SCR reaction, in relation to the specific questions formulated in the introduction, will be addressed in the subsequent paper.

ACKNOWLEDGMENTS

Financial support from the Netherlands agency for energy and the environment (NOVEM) and the Dutch Foundation for Chemical Research (SON) is gratefully acknowledged.

REFERENCES

1. Singoredjo, L., Korver, R. B., Kapteijn, F., and Moulijn, J. A., *Appl. Catal. B: Environ.* **1**, 297 (1992).
2. Singoredjo, L., Ph.D. thesis, University of Amsterdam, The Netherlands, 1992.
3. Kijlstra, W. S., Daamen, J. C. M. L., Van de Graaf, J. M., Van der Linden, B., Poels, E. K., and Bliek, A., *Appl. Catal. B: Environ.* **7**, 237 (1996).
4. Kapteijn, F., Singoredjo, L., and Moulijn, J. A., *Ind. Eng. Chem. Res.* **32**, 445 (1993).
5. Kijlstra, W. S., Poels, E. K., Bliek, A., Weckhuysen, B. M., and Schoonheydt, R. A., *J. Phys. Chem. B* **101**, 309 (1997).
6. Kapteijn, F., Singoredjo, L., Van Driel, M., Andreini, A., Moulijn, J. A., Ramis, and Busca, G., *J. Catal.* **150**, 105 (1994).
7. Kijlstra, W. S., Brands, D. S., Poels, E. K., and Bliek, A., *J. Catal.*, subsequent paper.
8. Topsøe, N.-Y., *Science* **265**, 1217 (1994).
9. Topsøe, N.-Y., Dumesic, J. A., and Topsøe, H., *J. Catal.* **151**, 241 (1995).
10. Rajadhyaksha, R. A., and Knözinger, H., *Appl. Catal.* **51**, 81 (1989).
11. Arakawa, T., Mizumoto, M., Takita, Y., Yamazoe, N., and Seiyama, T., *Bull. Chem. Soc. Jpn.* **50**, 1431 (1977).
12. Ramis, G., Yi, L., Busca, G., Turco, M., Kotur, E., and Willey, R. J., *J. Catal.* **157**, 523 (1995).
13. Ramis, G., Busca, G., Bregani, F., and Forzatti, P., *Appl. Catal.* **64**, 259 (1990).
14. Ito, E., Mergler, Y. J., Nieuwenhuys, B. E., Van Bekkum, H., and Van den Bleek, C. M., *Microporous Mater.* **4**, 455 (1995).
15. Centi, G., and Perathoner, S., *J. Catal.* **152**, 93 (1995).
16. Schneider, H., Scharf, U., Wokaun, A., and Baiker, A., *J. Catal.* **147**, 545 (1994).
17. Centi, G., and Perathoner, S., *Catal. Today* **29**, 117 (1996).
18. Komatsu, T., Ogawa, T., and Yashima, T., *J. Phys. Chem.* **99**, 13053 (1995).
19. Hadjiivanov, K. I., Klissurski, D. G., and Bushev, V. Ph., *J. Chem. Soc. Faraday Trans.* **91**, 149 (1995).
20. Kapteijn, F., Van Langeveld, A. D., Moulijn, J. A., Andreini, A., Vuurman, M. A., Turek, A. M., Jehng, J.-M., and Wachs, I. E., *J. Catal.* **150**, 94 (1994).
21. Singoredjo, L., Slagt, M., Van Wees, J., Kapteijn, F., and Moulijn, J. A., *Catal. Today* **7**, 157 (1990).
22. Bijsterbosch, J. W., Van Langeveld, A. D., Kapteijn, F., and Moulijn, J. A., *Vibr. Spectr.* **4**, 245 (1993).
23. Joly, J. P., Kjalfallah, M., Bianchi, D., and Pajonk, G. M., *Appl. Catal. A* **98**, 61 (1993).
24. Abello, M. C., Velasco, A. P., Gorriz, O. F., and Rivarola, J. B., *Appl. Catal. A* **129**, 93 (1995).
25. Tsyganenko, A. A., Pozdnyakov, D. V., and Filimonov, V. N., *J. Molec. Struc.* **29**, 299 (1975).
26. Peri, J. B., *J. Phys. Chem.* **69**, 231 (1965).
27. Knözinger, H., and Ratnasamy, P., *Catal. Rev. Sci. Eng.* **17**, 31 (1978).
28. Kapteijn, F., Singoredjo, L., Andreini, A., and Moulijn, J. A., *Appl. Catal. B: Environ.* **3**, 173 (1994).
29. Cerruti, L., Modone, E., Guglielminotti, E., and Borello, E., *J. Chem. Soc. Faraday Trans. I* **70**, 729 (1974).
30. Centi, G., Perathoner, S., Biglino, D., and Giamello, E., *J. Catal.* **151**, 75 (1995).
31. Davydov, A. A., "Infrared Spectroscopy of Adsorbed Species on the Surface of Transition Metal Oxides" (Rochester, Ed.), Wiley, New York, 1990.
32. Pozdnyakov, D. V., and Filimonov, V. N., *Kinet. Katal.* **14**, 655 (1973).
33. Schraml-Marth, M., Wokaun, A., and Baiker, A., *J. Catal.* **138**, 306 (1992).
34. Valyon, J., and Hall, W. K., *J. Phys. Chem.* **97**, 1204 (1993).
35. Dines, T. J., Rochester, C. H., and Ward, A. M., *J. Chem. Soc. Faraday Trans.* **87**, 1617 (1991).
36. Sacconi, L., Sabatini, A., and Gans, P., *Inorg. Chem.* **3**, 1772 (1964).
37. Eguchi, K., Watabe, M., Ogata, S., and Arai, H., *J. Catal.* **158**, 420 (1996).
38. Eguchi, K., Watabe, M., Ogata, S., and Arai, H., *Bull. Chem. Soc. Jpn.* **68**, 1739 (1995).
39. Ozkan, U. S., Cai, Y., and Kumthekar, M. W., *J. Catal.* **149**, 390 (1994).
40. Valyon, J., and Hall, W. K., *J. Catal.* **143**, 520 (1993).
41. Ozkan, U. S., Kumthekar, M. W., and Cai, Y. P., *Ind. Eng. Chem. Res.* **33**, 2924 (1994).
42. Niiyama, H., Murata, K., Can, H. V., and Echigoya, E., *J. Catal.* **62**, 1 (1980).
43. Boreskov, G. K., *Advan. Catal.* **15**, 285 (1964).
44. Chang, Y., and McCarty, J. G., *J. Catal.* **165**, 1 (1997).
45. Li, Y., and Armor, J. N., *Appl. Catal.* **76**, L1 (1991).
46. Eränen, K., Kumar, N., and Lindfors, L.-E., *Appl. Catal. B: Environ.* **4**, 213 (1994).
47. Hierl, R., Urbach, H.-P., and Knözinger, H., *J. Chem. Soc. Faraday Trans.* **88**, 355 (1992).
48. Sadykov, V. A., Baron, S. L., Matyshak, V. A., Alikina, G. M., Bunina, R. V., Rozovskii, A. Ya., Lunin, V. V., Lunina, E. V., Kharlanov, A. N., Ivanova, A. S., and Veniaminov, S. A., *Catal. Lett.* **37**, 157 (1996).